SECURITY CLASSIFICATION OF THIS PAGE (When Data Entered)

AD A109037

DTIC FILE COPY

REPORT DOCUMENTATION PAGE

READ INSTRUCTIONS BEFORE COMPLETING FORM

1. REPORT NUMBER AFOSR-TR- 81 -0865	2. GOVT ACCESSION NO. AD-A109 037	3. RECIPIENT'S CATALOG NUMBER
4. TITLE (and Subtitle) CATOPTRIC X-RAY OPTICAL SYSTEM (For Use in Laser-Fusion Diagnostics)		5. TYPE OF REPORT & PERIOD COVERED Annual Technical Report Oct. 1, 1980-Sept. 30, 1981
		6. PERFORMING ORG. REPORT NUMBER
7. AUTHOR(s) Professor James F. McGee		8. CONTRACT OR GRANT NUMBER(s) AFOSR 78-3480
9. PERFORMING ORGANIZATION NAME AND ADDRESS Department of Physics Saint Louis University 221 N. Grand Blvd., St. Louis, MO 63103		10. PROGRAM ELEMENT, PROJECT, TASK AREA & WORK UNIT NUMBERS 61102F 2301-A7
11. CONTROLLING OFFICE NAME AND ADDRESS Air Force Office of Scientific Research Building 410 Bolling AFB, DC 20332		12. REPORT DATE November 30, 1981
		13. NUMBER OF PAGES 20
14. MONITORING AGENCY NAME & ADDRESS(if different from Controlling Office)		15. SECURITY CLASS. (of this report) Uncl
		15a. DECLASSIFICATION/DOWNGRADING SCHEDULE

LEVEL II

16. DISTRIBUTION STATEMENT (of this Report)

Approved for public release; distribution unlimited.

17. DISTRIBUTION STATEMENT (of the abstract entered in Block 20, if different from Report)

DTIC ELECTE DEC 31 1981 S D H

18. SUPPLEMENTARY NOTES

19. KEY WORDS (Continue on reverse side if necessary and identify by block number)

X-RAY OPTICS

LASER DIAGNOSTICS

20. ABSTRACT (Continue on reverse side if necessary and identify by block number) A compound x-ray imaging device is being developed as an aid in the diagnostics of a laser-fusion process which involves a pellet about 100 microns in diameter. While previous reports have dealt with the use of certain aspheric surfaces in the x-ray imaging process, this report is confined to a thorough investigation of the use of Abbe's sine condition at grazing angles of incidence in the case of a single reflector.

DD FORM 1 JAN 73 1473

Uncl 323875

SECURITY CLASSIFICATION OF THIS PAGE (When Data Entered)

TABLE OF CONTENTS

	Cover and Title Page (DD Form)	i
	Table of Contents	ii
I.	Introduction	1
	Significance and Principal Aim of the Research	
II.	Recent Work by the Principal Investigator and Students . . .	2
	A. Coma Reduction in the Single X-Ray Reflector	2
	1. Application to a Spherical Mirror	5
	2. An Extended Sine Relationship with Application to Reflection at Grazing Incidence	7
	3. Comparison of Ray Tracings for an Old and a New Selection of Parameters	12
III.	Cumulative Publications	15
IV.	References	15
V.	Biographical Sketches	16

I. Introduction:

A. Significance and Principal Aim of the Research

For some time now the need for a good scheme to image the x-rays associated with the laser-fusion implosion process of a thin spherical pellet in the 50 to 100 micron diameter range has been evident. Several laboratories have resorted to the age old pin-hole camera (literally a pin-hole in a sheet of lead which is positioned between the source and the recording film). Its quoted resolution of 15 microns by one source leaves much to be desired. A resolution at least two orders of magnitude lower would be desirable and attainable by x-ray focusing methods.

The principal investigator built the first successful long-wavelength x-ray microscope at Standord while working under Professor Kirkpatrick. The microscope was capable of making x-ray micrographs of biological tissue-sections only seven microns thick with adequate contrast. In those days a detailed knowledge of the geometrical and physical optics connected with the formation of images by the total-external reflection of x-rays was only in its infancy, this particular phase of optics never having attracted the attention of the great optical scientists of bygone days.

Crossed-mirror x-ray microscopes as used by the author and others have been of the simple magnifier type. They lacked an ocular or eyepiece lens found in the ordinary compound light-microscope so common to biological laboratories. A compound microscope either for light or x-rays would be distinguished from a simple magnifier by the formation of an intermediate image.

Crossed-mirror x-ray microscopes have been used as simple magnifiers with one important difference. The object was placed just outside the first focal point so as to form a real magnified image which could be recorded on film.

We propose then the study and construction of a compound reflection x-ray system which will have sufficient resolution and magnification for laser fusion diagnostic purposes in the wavelength region of approximately 5 to 50 Å.

The compound x-ray microscope could be operated so that the real image formed by the objective lens would fall just outside of the focal point of the ocular or second lens so that the latter would produce a real image which could be recorded on film or by a vidicon or CCD.

Ordinarily we think of a telescope as an instrument which is used to examine large objects (moon) at large distances (moon to earth). A microscope on the other hand is used to examine small objects (a bacterium) at small distances (oil-immersion lens). The pellet used in laser fusion is indeed small (50 to 100 microns). However it is not feasible to examine it at very small distances, as it implodes, because of possible damage to the observing system from target debris and heat. With the latter realization the goal is modified to that of examining a small object at a large distance. Occasionally biologists are faced with a similar need and will exchange their objective lens having a focal length of a fraction of a mm for one which has a focal length of 5 cm. The latter type of objective lens is referred to as a "large working distance" objective since now the specimen must be placed slightly greater than 5 cm from the objective lens.

A suitable x-ray imaging system for laser fusion diagnostics does indeed need an objective lens with a "large working distance". For instance in the Rochester tank no diagnostic apparatus can be closer than 22 cm to the target. Even more serious than this mechanical limitation is the fact that at calculated power output aluminum filter-foils would be vaporized and optical components otherwise damaged by target debris.

Due to the heating and debris constraints we are currently designing our apparatus so that no parts project within the tank. Our design working-distance will be 90 to 100 cm subject to change of course upon receipt of further information. The Rochester tank is 90 cm in radius with many ports about 5.08 cm in diameter.

II. Recent Work by the Principal Investigator and Students

A. Coma Reduction in the Single X-Ray Reflector

A reduction of the amount of coma in an optical system implies that Abbe's sine condition is being satisfied to some extent. It is well known that if an axial point is imaged without spherical aberration it does not follow that a point slightly off-axis will be imagined free of spherical aberration. When an off-axis point exhibits spherical aberration, the geometrical aberration present is known as coma. Abbe's sine condition as stated and sometimes derived in standard optics textbooks refers to refraction optics. While admittedly not a perfect condition, the usual admonition is to keep the object and image size small. It is not clear with what the image or object size should be compared.

As previously stated Abbe's sine condition is derived for the refraction case. What if any changes in its form or interpretation occur in the case of reflection-optics and in particular, grazing incidence optics at x-ray wavelengths?

It will be helpful to review some historical geometrical methods of following the path of a ray refracted at a spherical surface before proceeding to the reflection case at grazing incidence. Thomas Young[1] provides an interesting geometrical construction for the path of a ray refracted at a spherical surface.

In Fig. 1 the center of the spherical refracting surface S of radius r is designated by C. Its index of refraction is n' where n' > n. Let PB represent the incident ray direction. Next draw a circle of radius $\tau' = \frac{n}{n'} r$, concentric with the spherical refracting surface S. Finally, draw a similar concentric circle of radius $\tau = \frac{n'}{n} r$. Extend the line PB until it intersects the surface τ in Z, then join Z to C by a straight line and let Z' be the point of intersection of the latter with the surface τ'. The straight line

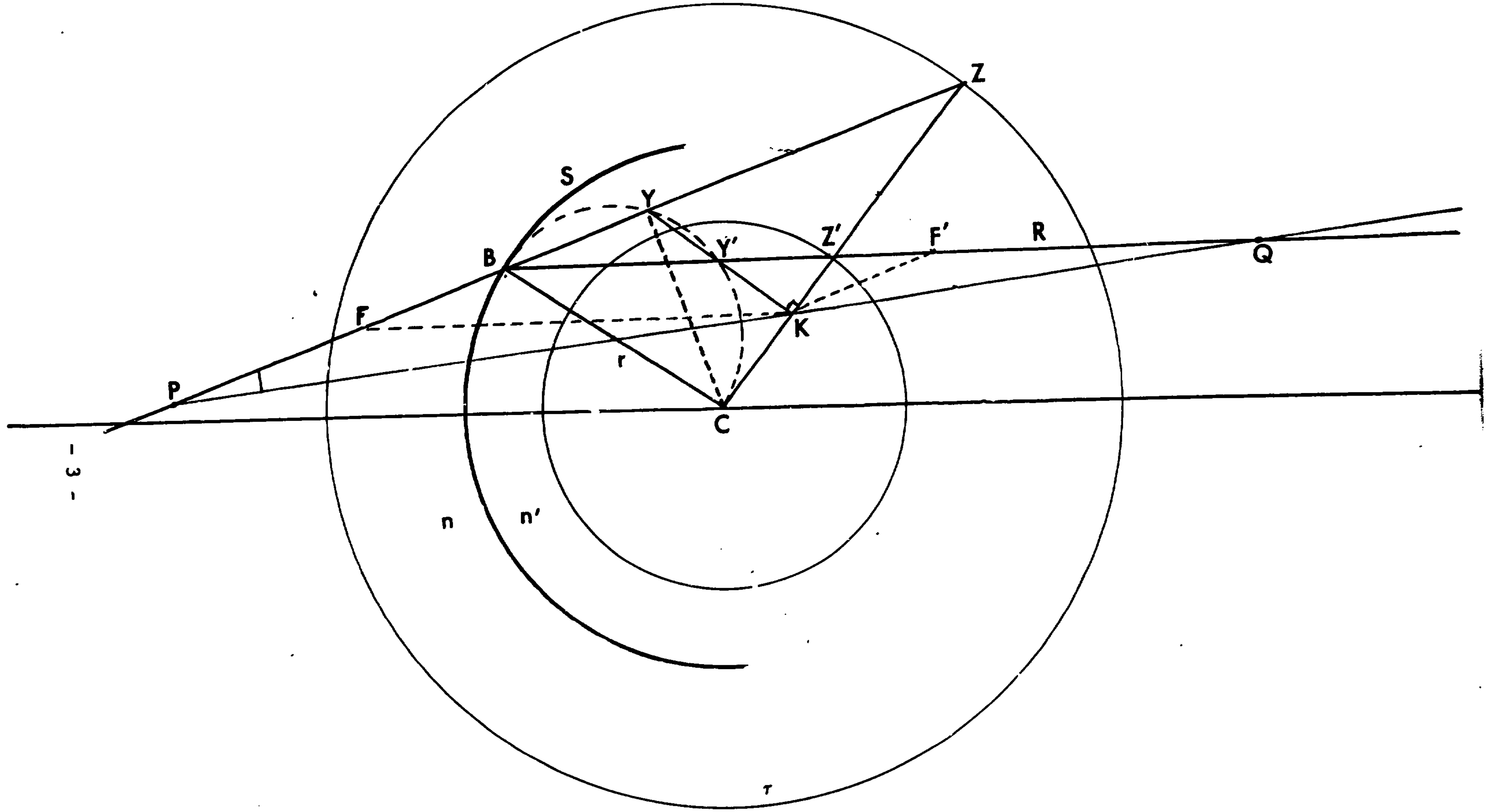

Fig. 1

drawn from B through Z' then gives the direction of the refracted ray BR'. Nc in Fig. 1 that

$$\frac{CZ}{CB} = \frac{CB}{CZ'} \tag{1}$$

Since the triangles CBZ and CBZ' are similar, $\angle CBZ = \angle BZ'C = \alpha$ and $\angle CBZ' = \angle BZC = \alpha'$. By the laws of sines:

$$\frac{CZ}{\sin\alpha} = \frac{CB}{\sin\alpha'} \quad \text{and} \quad \frac{CB}{\sin\alpha} = \frac{CZ'}{\sin\alpha'}$$

whence

$$\frac{CZ}{CB} = \frac{\sin\alpha}{\sin\alpha'} \quad \text{and} \quad \frac{CB}{CZ'} = \frac{\sin\alpha}{\sin\alpha'} \tag{2}$$

By the law of refraction:

$$\frac{\sin\alpha}{\sin\alpha'} = \frac{n'}{n} \tag{3}$$

Thus from Eqs. (1), (2), and (3)

$$\frac{CZ}{CB} = \frac{CB}{CZ'} = \frac{n'}{n} \tag{4}$$

which establishes the fact that BZ' is the path of the refracted ray.

In order to find the image-point Q from the position of its object-point P, the following additional construction on Fig. 1 is necessary. On BC as diameter construct a semi-circle meeting the chief incident ray PBZ in a point Y and the chief refracted ray BZ' in a point Y'. The so-called Center of Perspective K is determined by the intersection of the straight lines YY' and ZZ'. Since $\angle CBZ' = \angle CYY'$, both being inscribed angles standing on the same arc CY', it follows that YY' is perpendicular to CZ'Z at K. In virtue of the above, the following simple construction is made possible. Instead of drawing the semi-circle simply drop a perpendicular line from C to the incident ray direction (extended). Label the intersection Y. Next draw YK perpendicular to CZ at K. Finally the straight line from P through K will intercept the refracted ray BZ' at the image point Q. The points Z and Z' have the interesting property that to a homocentric bundle of incident rays converging to Z corresponds a homocentric bundle of refracted rays converging to Z'. The latter property is independent of the angular opening of the incident bundle of rays and hence is true for a finite aperture. The pair of conjugate points Z and Z' which lie on the axis of a spherical surface as shown in Fig. 1 are called an "aplanatic pair" for which the spherical surface is aberrationless.

Still another viewpoint of the aplanatic pair of points Z and Z' is to note that since $CZ' = \frac{n}{n'} r$ and $CZ = \frac{n'}{n} r$ the product

$$CZ \cdot CZ' = r^2 \tag{5}$$

which reminds one of the solution of certain electrostatic problems by "inversion in a sphere".

The points Z and Z' always lie on the same side of the center C of the spherical refracting surface with the consequence that the real rays pass through one point Z and the extrapolated rays will form a virtual image at Z'. Thus one of the spherical surfaces τ is the virtual image of the other surface τ'.

1. Application to a Spherical Mirror

It is not unusual in optical treatment to make a derivation for the refracting case and then apply the result to the reflection case by simply setting $n' = -n$.

By referring to Fig. 2, the law of refraction is given by

$$n' \sin \alpha' = n \sin \alpha \quad . \tag{6}$$

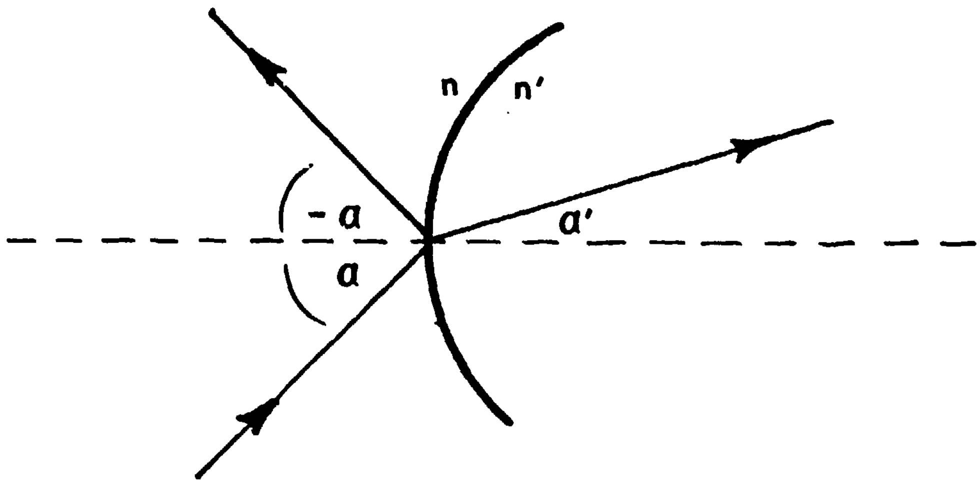

Fig. 2

In order that the latter formula be applicable to the case of reflection as well as refraction, the values of n' and n in the former case must be such that $\alpha' = -\alpha$. Therefore

$$n' \sin(-\alpha) = n \sin \alpha$$

hence

$$n' = -n, \text{ the stated requirement.}$$

However, in the case of reflection at a spherical mirror the previous construction fails since

$$CZ' = \frac{n}{n'} r \quad \text{becomes} \quad CZ' = -r$$

and

$$CZ = \frac{n'}{n} r \quad \text{becomes} \quad CZ = -r \quad .$$

Thus a spherical mirror has no pair of "aplanatic points" corresponding to Z and Z'. From the relation

$$\frac{CZ}{CB} = \frac{CB}{CZ'} = \frac{n'}{n} = \frac{(-n)}{n} = -1 \tag{7}$$

it follows that CB = -CZ' and CB = CZ. In other words, the aplanatic points Z and Z' coincide at the vertex of the mirror and hence do not exist as separate points as in the case of refraction.

Although in the case of reflection at the surface of a mirror we cannot make use of the aplanatic points Z and Z' since they have no meaning, a similar construction for the reflection case is however possible[2] in the following manner as illustrated by Fig. 3.

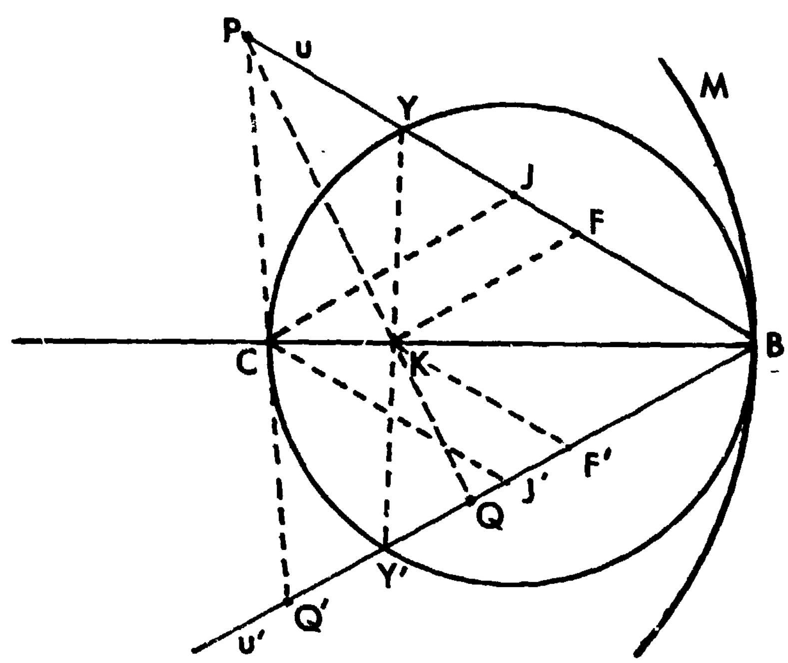

Fig. 3

In Fig. 3 the center of the spherical mirror M is designated by C. Let an incident ray μ meet the mirror at point B and be reflected as μ' so that $\angle CB\mu = \angle \mu' BC$. On CB as diameter construct a circle which cuts μ and μ' in the points Y and Y' respectively. Obviously as was the case in refraction, the point Y' on μ' is the image of the object point Y on μ and YY' intersects CB at the center of perspective K. To determine the image position of the meridian ray draw a straight line from the object point P on μ through the center of perspective point K to intersect the reflected ray μ' in Q. To determine the image position for a sagittal ray draw a straight line from the object point P on μ through the center C of the mirror circle to intercept the reflected ray in Q'.

Also it should be noted that straight lines drawn through K and C parallel to the incident ray μ will determine by their intersections with the reflected ray μ' the focal points of the meridional and sagittal rays F' and J' respectively. The conjugate focal points are determined by drawing through K and C lines parallel to the reflected ray μ' and noting their intersection with the incident ray μ. These points are already shown in Fig. 1 as F and F' respectively for focusing in the meridian plane.

2. An Extended Sine Relationship with Application to Reflection at Grazing Incidence

In Fig. 4 a concave reflector with its apex at B and of radius R has points Y and Y' already determined as in Fig. 3 for incoming and outgoing ray directions μ and μ' respectively. The center of perspective is at K. In Fig. 4 P and P' are conjugates as well as Γ and Γ' with Γ and Γ' on a pseudo-axis $\Gamma K \Gamma'$ which is at a very small distance KB from the vertex B. Since CY is perpendicular to μ and YKY' is perpendicular to CB it is easy to show that $CK = R \sin^2 \alpha$ and consequently $KB = R(1 - \sin^2 \alpha)$ which is very small for the case of grazing incidence where α approaches 90°. If in Fig. 4 the distance PB = p the object distance and BP' = q the image distance then since the triangles PFK and KF'P' are similar, the ratio of corresponding sides results in

$$\frac{p - f}{f'} = \frac{f}{v - f'} \tag{8}$$

where f = FB and f' = BF' respectively. Equation (8) upon cross multiplication becomes

$$(p - f)(v - f') = ff' \tag{9}$$

which is recognized as Newton's Equation in optics. By substituting $f' = f = (R \sin i)/2$, the well known focal length in the meridian plane for grazing incidence, where $i = (90° - \alpha)$ of Fig. 4 and R is the radius of curvature of the reflecting surface, Newton's equation reduces to

$$\frac{1}{p} + \frac{1}{q} = \frac{2}{R \sin i} \tag{10}$$

the equation commonly used to determining image formation at grazing angles of incidence in the meridian plane.

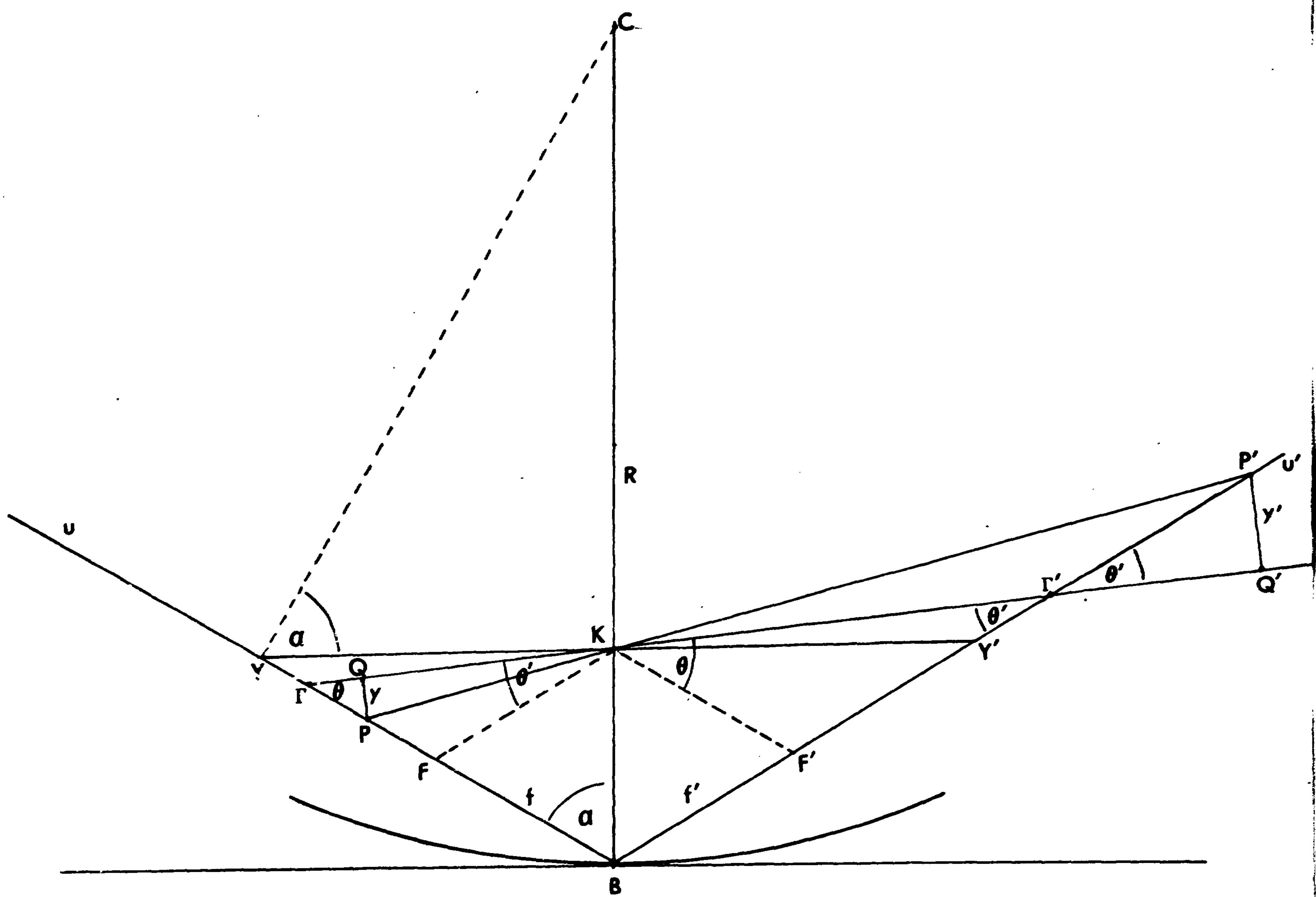

Fig. 4

For point P in Fig. 4 the distance $(p - f)$ is given by

$$(p - f) = PF = \Gamma F - \Gamma P \tag{11}$$

and the distance $(q - f)$ is given by

$$(q - f) = F'P' = F'\Gamma' + \Gamma'P' \ . \tag{12}$$

By construction

$$PQ = y = \Gamma P \sin\theta \tag{13}$$

and

$$P'Q' = y' = \Gamma'P' \sin\theta \tag{14}$$

Also note that by the law of sines

$$\frac{\Gamma F}{\sin\theta'} = \frac{f'}{\sin\theta} \tag{15}$$

and

$$\frac{\Gamma'F'}{\sin\theta} = \frac{f}{\sin\theta'} \tag{16}$$

With $f = f'$ for the reflection case, substitution in Eq. (9) yields

$$f^2 = (\Gamma F - \Gamma P)(\Gamma'F' + \Gamma'P') \tag{17}$$

which becomes upon substituting from Eqs. (13), (14), (15), and (16)

$$f^2 = \left[f\,\frac{\sin\theta'}{\sin\theta} - \frac{y}{\sin\theta}\right]\left[f\,\frac{\sin\theta}{\sin\theta'} + \frac{y'}{\sin\theta'}\right] \tag{18}$$

Upon dividing by f and rearranging the result is

$$y' \sin\theta' - y \sin\theta = \frac{yy'}{f} \ . \tag{19}$$

Equation (19) will be referred to as the <u>extended sine condition</u> for grazing incidence optics.

Abbe sine condition as usually stated for refraction optics is

$$n'y' \sin\gamma' - ny \sin\gamma = 0 \tag{20}$$

where n and n' are the refractive indices of object and image space respectively and γ and γ' are the angular apertures for an object and image point respectively. Since the product of a refraction index and a geometrical distance is an optical path length, Abbe's sine condition implies the application of Fermat's principle in its derivation and thus requires for good imaging that the difference between some two optical paths be exactly zero. Previous applications of the zero form of Abbe's sine condition would rule out the possibility of using a single reflector for good imaging free of coma.

The high quality of some experimental x-ray images using single reflecting surfaces raised some questions about the interpretation and limits of Abbe's sine condition as commonly stated and applied. The final Eq. (19) specifies the condition under which a good image can be obtained with a predetermined amount of wave-front aberration. The index of refraction does not occur in Eq. (19), the extended sine condition, since it is unity in the case of reflection.

The form of Eq. (19) lends itself to a ready determination of what object sizes can be tolerated for a given magnification and focal length of a single reflector system for a given error ε in optical path. Rewriting Eq. (19) for small angles and error ε

$$y'\theta' - y\theta + \varepsilon = \frac{yy'}{f}$$

Dividing by y

$$\frac{y'}{y}\theta' - \theta + \frac{\varepsilon}{y} = \frac{yy'}{yf}$$

Defining $y'/y \equiv M$, the magnification, then

$$M\theta' - \theta + \frac{\varepsilon}{y} = \frac{My}{f}$$

Also, since $M = \theta/\theta'$ and $\theta = M\theta'$ the result is

$$M = \frac{\varepsilon f}{y^2} \tag{21}$$

Thus if we are satisfied with an error $\varepsilon = \lambda/4$ of wave aberration

$$M = \frac{\lambda f}{4y^2} \tag{22}$$

Typically a system with a focal length of f = 4 cm would give an image good to the indicated tolerance if the object is 4 microns high and the magnification = 343.8 using λ = 5500 Å. For a focal length of f = 8 cm and an object height of 32 microns the magnification should be 10.74.

The formula has been calculated for a variety of focal lengths and object sizes the results of which are shown in Table 1. All were calculated using λ = 5500 Å. Since we are ultimately dealing with x-rays it might seem strange to use an error which is a fraction of a wavelength of visible light. Remember that we are dealing with wave-front aberrations which cause a displacement of the intersection of an x-ray pencil with the recording film. The transverse displacement on the film would only become bothersome when the wave-front error is measured in fractions of a visible light wavelength.

Various derivations of Abbe's sine condition assume that the imaging of an axial point is free of spherical aberration and then proceed to apply

$\bar{f}$ (cm)

y microns	1	2	4	8	16	32	64	128	256	512	1024	
1	1375	2750	5500	11000	22000							
2	343.75	687.5	1375	2750	5500	11000	22000					
4	85.94	171.88	343.8	687.5	1375	2750	5500	11000	22000			
8	21.48	42.97	85.94	171.88	343.7	687.5	1375	2750	5500	11000	22000	
16	5.37	10.74	21.48	42.97	85.94	171.88	343.8	687.5	1375	2750	5500	11000
32	1.34	2.69	5.37	10.74	21.48	42.97	85.94	171.88	343.8	687.5	1375	2750
64	0.34	0.67	1.34	2.68	5.37	10.74	21.48	42.97	85.94	171.88	343.7	687.5
128			0.34	0.67	1.34	2.69	5.37	10.74	21.48	42.97	85.94	171.88
256					0.34	0.67	1.34	2.68	5.37	10.74	21.48	42.97
512							0.34	0.67	1.34	2.68	5.37	10.74
1024									0.34	0.67	1.34	2.68

"M"

MAXIMUM MAGNIFICATION

(for a $\lambda/4$ of wave-aberration)

Table 1

Fermat's principle to arrive at the commonly stated form. The previous derivation of the extended sine condition suffers from the same defect and leads one to expect that the imaging could be further improved by using a slightly aspheric surface. Previous ray-tracing involving sophisticated aspheric-surfaces, did not always show good results because, as it is now realized, the selected parameters such as radius of curvature, angle of grazing incidence, object and image distances, extent of object, did not agree with the tolerable values stated in Table 1.

On one or two occasions the experimental images were better than expected. They can now be almost completely explained by the fact that the correct parameters according to Eq. (21) were accidently selected due to constraints on the equipment and positioning of some of the components in laboratory space.

3. Comparison of Ray Tracings for an Old and a New Selection of Parameters

After incorporating Abbe's sine condition as commonly used in the design of several x-ray optical systems, it was found, upon ray tracing, that the results were disappointing in spite of keeping the object and image size small as recommended in several textbook versions of Abbe's sine condition. One perceived difficulty in its application is with what should the smallness of the object and image size be compared. Also, what is an allowable tolerance for satisfactory imaging. These questions are more satisfactorily answered by the use of the extended sine condition as developed for grazing incidence optics in the preceeding section.

As seen by Table 1 and Eq. (21), once a tolerance such as a quarter wavelength of wave-front error has been decided upon, the selection of any two of the three parameters y, f and M fixes the value of the third. The remaining parameters are then easily found. For example, since $f = R \sin i/2$ and i is usually the maximum attainable i for the wavelength of x-rays in use and the material of the reflector surface, R is determined. The selection of the image distance q follows that of the object distance p since the latter must be chosen to be greater than f if a real image is to be formed.

A somewhat dramatic indication of the usefulness of the extended sine condition may be seen in its application to a single reflector. In the past, it has not been uncommon for one to dismiss the possibility of forming good x-ray images by a single reflector system. The usual stated reason was that a single-reflector could not be made to satisfy Abbe's sine condition. That something was being overlooked became obvious when occasionally a good x-ray image would turn up experimentally.

In what follows a comparison will be made between the resulting images governed by the extended sine condition with respect to the original selection of parameters and an image resulting from a selection of parameters which have been determined by outside requirements such as distance to target in the laser-fusion experiment or parameters which have been "dreamed" up for the sake of a numerical calculation.

In Fig. (5) the results of two determinations of intensity distributions in the image plane are superimposed. Before superpositioning, each intensity distribution was divided by its magnification. This procedure makes any alteration of the object by the imaging system readily apparent. Ideally, of course, the image, reduced by its magnification, should be an exact replica of the object but practical systems never yield such a result. Intensity, as used in this context, refers to the number of rays from an object point which intersect the Gaussian image plane within some previously assigned "cell" length. This geometrical intensity definition, of course, would break down in the case of perfect point-to-point imaging since the intersections with the image plane would be considerably less than a wavelength.

For the intensity distribution shown as solid black lines in Fig. (5) the parameters $f = 80$ cm, $y = 100$ microns and $M = 10$ were chosen to be in reasonably close agreement with Eq. (22) which would yield $M = 11$ for the desireable magnification. From each of six object points, separated a distance of 20 microns, a thousand rays were followed through the system and their intersections with the corresponding image plane determined. Some 200 cells each 5 microns wide in image space were used to collect the rays. For the image shown as heavy dark lines in Fig. (5), all 1000 rays from each object point fell in a single cell in image space which translates into 0.5 microns of maximum width in object space.

The latter intensity distribution is to be compared with that of a system whose parameters were originally selected without knowledge of the extended sign condition expressed by Eq. (22). The cross-hatched distribution shown in Fig. (5) is for a system whose focal length $f = 2.90$ cm, $y = 500$ microns and $M = 30$. Since the object points in this case were 100 microns apart the only overlap with the first case occurs at $y = 0$ and $y = 100$ microns. It is noted that for the field point at $y = 100$ microns, the image when referred to object space is spread over 9 microns. Although not shown in Fig. (5), the situation becomes worse at $y = 200$ microns, where the reduced image-width is 12 microns in object space.

These results and others at hand would seem to bear out the thesis that the single x-ray reflector has very useful qualities when the operating system parameters are carefully selected to closely satisfy the extended sine condition as represented by Eq. (21).

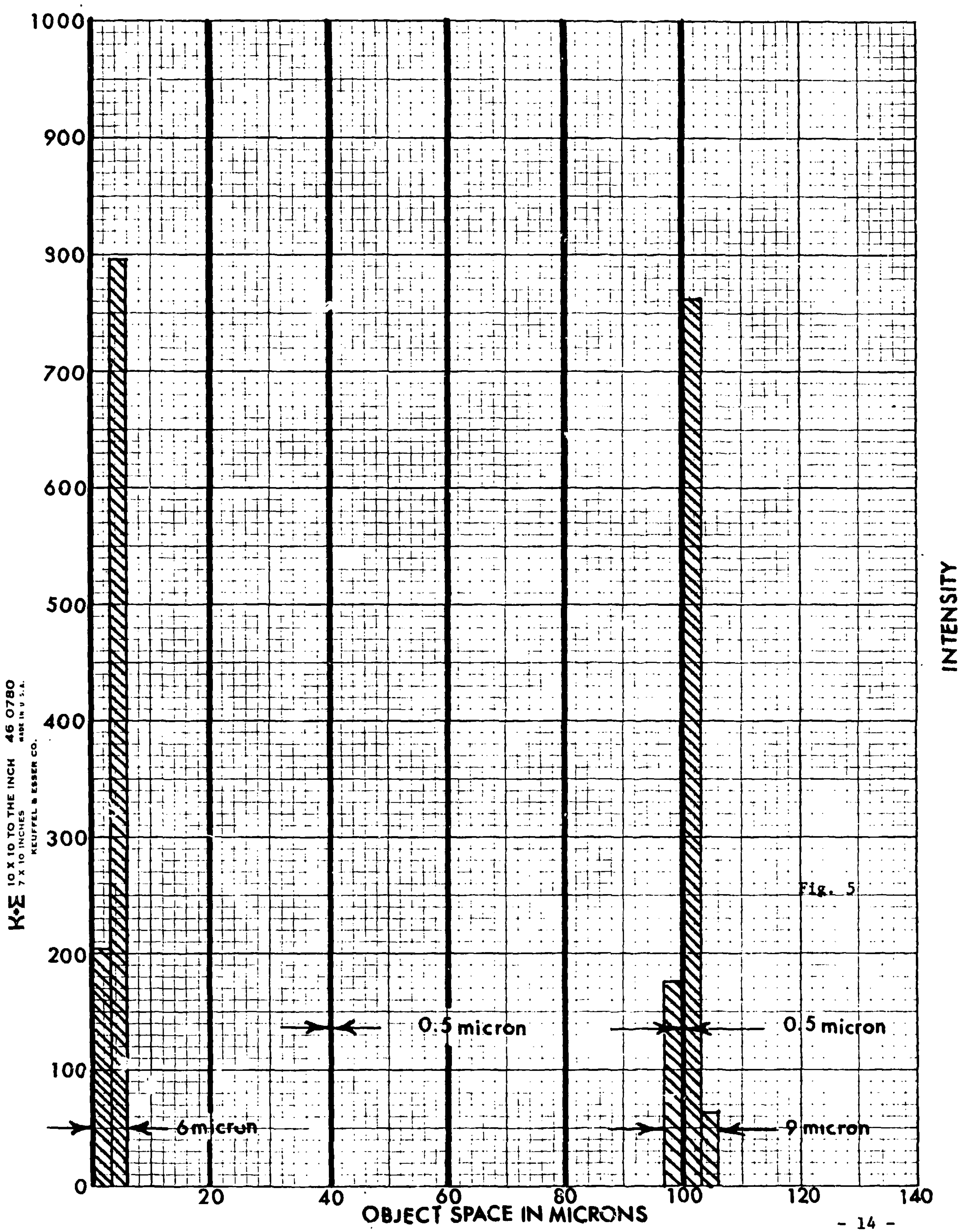
INTENSITY
OBJECT SPACE IN MICRONS
0
100
200
300
400
500
600
700
900
900
1000
20
40
60
80
100
120
140
6 micron
0.5 micron
0.5 micron
9 micron
K+E 10 X 10 TO THE INCH 7 X 10 INCHES KEUFFEL & ESSER CO. 46 0780 MADE IN U.S.A.
Fig. 5

III. Cumulative Publications

A Low-Budget Cylindrical-Surface Generator in "Workshop on Optical Fabrication and Testing," a Technical Digest by the Optical Society of America 1980.

A Plasma Controlled X-Ray Tube in Vol. 22 "Advances in X-Ray Analysis," Plenum Press, New York 1980.

Properties of an X-Ray Catoptric System in Vol. 190, "Los Alamos Conference on Optics '79," published by SPIE, Washington 1979.

IV. References

1. A Course of Lectures on Natural Philosophy and the Mechanical Arts, by Thomas Young, London 1807, Vol. II, page 73 Art. 425.

2. Principles and Methods of Geometrical Optics by James P. C. Southall, Macmillian Company, London 1910, page 362.

Biographical Sketch

Name

McGee, James F.

Title

Professor

Place of Birth

Philadelphia, Pennsylvania

Nationality

U.S.A. Citizen

Sex

Male

Education

B.S.	1938	Physics	St. Joseph's College, Philadelphia, Pa.
M.S.	1940	Physics	University of Notre Dame, Indiana
Ph.D.	1956	Physics	Stanford University, California

Honors

Fulbright Professor of Physics, Finland, 1964-65
President, Sigma Xi (Saint Louis Chapter), 1968-69
Gold Medal for Mathematics, St. Joseph's College

Major Research Interest

X-Ray Optics

Role in Proposed Project

Principal Investigator

Research Support

Previous: Research Corporation, National Science Foundation, American Cancer Society, and National Institutes of Health

Current: Air Force Office of Scientific Research

Research and/or Professional Experience

1969-present	Professor of Physics, Saint Louis University
1959-1969	Associate Professor, Saint Louis University
1956-1959	Assistant Professor, Saint Louis University
1955-1956	Research Associate, Stanford University
1952-1955	Research Assistant, Stanford University
1949-1952	Research Engineer, Atomics International Division of North American Aviation, now Rockwell International
1946-1949	Research Engineer, Aerophysics Division of North American Aviation, now Rockwell International

Biographical Sketch

Name	Title	
Ritva A.M. Keski-Kuha	Research Assistant	
Place of Birth	**Nationality**	**Sex**
Finland	Finnish	Female

Education

B.S.	1976	Physics	University of Turku, Finland
M.S.	1977	Physics	University of Turku, Finland

Major Research Interest	Role in Proposed Project
X-Ray Optics	Research Assistant

Research and Professional Experience

1978-79	Research Assistant	Saint Louis University	Research
1977-78	Research Assistant	University of Turku	Research & Teaching

Publications

1. "Total Reflection of X-Rays from the Transition Metals Fe, Cu, and Co Close to Their L-Absorption Edges," Proceedings of the Annual Conference of the Finnish Physical Society, 1978.

2. "X-Ray Reflectivity of Cobalt and Titanium in the Vicinity of the $L_{2,3}$ Absorption Edges," J. Bremer, L. Kaihola and Ritva Keski-Kuha in the Journal of Physics C: Solid State Physics. (Accepted for publication 13 August 1979.)

Biographical Sketch

Name	Title	
Timo T. Saha	Research Assistant	
Place of Birth	**Nationality**	**Sex**
Finland	Finnish	Male

Education

B.S.	1974	Physics	University of Turku, Finland
M.S.	1975	Physics	University of Turku, Finland

Major Research Interest	Role in Proposed Project
X-Ray Optics	Research Assistant

Research and Professional Experience

1978-79	Research Assistant	Saint Louis University	Research & Teaching
1977-78	Research Assistant	University of Turku	Research & Teaching
1974-75	Research Assistant	University of Turku	Research & Teaching

Publications

1. "Electron Microscope Analysis of Epitaxially Grown Fe_2O_3 Crystals," Proceedings of the Annual Conference of the Finnish Physical Society, 1977.

2. "A Plasma Controlled X-Ray Tube," J. F. McGee and Timo Saha in Vol. 23, Advances in X-Ray Analysis, edited by J. R. Rhodes, C. S. Barrett and J. B. Newkirk, Plenum Press, New York, 1980.